

ARTICLE OPEN



Future temperature-related hospitalizations from cardiovascular diseases among rural residents in southeastern China considering population aging

Zhi-Ying Zhan^{1,6}, Jun Yang^{2,6}, Xue Zhong^{1,6}, Xiao-Xu Xie¹, De-Li Liu^{3,4}, Zhen-Quan Zheng⁵ and Zhi-Jian Hu¹✉

Future climate changes are projected to adversely affect mortality risk of cardiovascular disease (CVD) in urbanized regions. However, future temperature-related excess CVD hospitalizations in rural residents with poorer socioeconomic status is not well understood. Moreover, influence of aging and declining rural population are rarely considered. Using CVD hospitalizations in rural residents during 2010–2016 in eight regions in southeastern China, the region-specific temperature-CVD associations were estimated by generalized additive models, which were combined by a meta-regression. We projected excess CVD hospitalizations due to temperature using regional associations for 27 climate models under scenarios of climate change for 2010–2099. To reveal the influences of aging and declining rural population, age-specific associations and future population change ratio were used to estimate age-specific number of temperature-related hospitalizations. We found that heat-related hospitalizations in rural residents from ischemic stroke, ischemic heart disease and cerebrovascular disease are projected to increase in the 2090 s, although the excess CVD hospitalizations associated with future temperature in rural residents will reduce in the 2090 s. Rural population aging amplifies temperature-related CVD burden by >2.34-fold under SSPs in the 2050 s compared to scenarios with only population declining, although rural population reduction will reduce the temperature-related CVD hospitalizations in the 2090 s. The elderly, male and those lived in Longyan and Sanming could be more affected. These findings suggest that future heat is projected to increase hospitalizations of some CVD subcategories. Policies are needed to mitigate increasing temperature and baseline hospitalization rate. The impact of population aging is noteworthy.

npj Climate and Atmospheric Science (2023)6:112; <https://doi.org/10.1038/s41612-023-00439-7>

INTRODUCTION

Globally, there were 17.9 million deaths due to CVD in 2016, accounting for 32% of all deaths¹. In 2030, The CVD is projected to be the cause of >23.0 million deaths². Meanwhile, CVDs accounted for 24% of all hospital admission among middle-aged people from 21 countries, and accounted for 59% in the developing countries³. In China, the prevalence of CVD is serious and continues to rise, and the death rate is higher in rural regions than that in urban regions⁴.

Ongoing climate change has received increasing attention, characterized by increasing surface temperature⁵. Previous studies collected and analyzed historical data, and suggested that warmer temperatures may increase the hospital admission from CVD and its subcategories⁶. Moreover, the global surface temperature is predicted to increase between 2.6 °C and 4.8 °C from 1986–2005 to 2081–2100 under high-emission scenarios, which may contribute to an increased incidence of CVD in future. Thus, projecting potential influence of continued warming in the future is critical for policymakers to develop mitigation initiatives to minimize future CVD burden.

Current studies have focused on projections of CVD deaths related to future non-optimal temperature in highly developed urban areas^{7,8}, resulting in considerable uncertainties when generalizing the evidence to morbidity (i.e. hospital admission) or to regions with diverse socioeconomic levels. In the context of

global warming and frequent heat events, heat-related excess mortality is projected to increase in China, especially among the population in the southeastern region, with cardiovascular disease, or with lower levels of education^{7,9}. However, there is a lack of evidence regarding the projections of excess CVD hospital admission attributable to future temperature among rural residents, those with poorer socioeconomic level and lower level of education. Moreover, previous studies were limited to project potential influence of increasing temperature on total CVD^{7,8,10}, and very limited evidence on its common subcategories, such as ischemic heart disease and stroke¹¹. Further studies are needed to project temperature-related hospital admissions from different cause-specific CVDs. Third, the current studies have mainly reported the excess CVD related to future temperature in a short-time period within the 2010 s–2070 s^{10–12}, but few studies clearly revealed the trend in a long-time period. It is known that older adults with poor physiological and social condition are particularly vulnerable to climate change. However, although population aging is accelerating globally due to lower fertility rates and longer life expectancies¹³, the change of rural population structure and size have not been adequately accounted for in projection of temperature-related health burden¹⁴.

The existing evidence based on the future temperature from only a few climate models have not adequately described the

¹Department of Epidemiology and Health Statistics, Fujian Provincial Key Laboratory of Environment factors and Cancer, School of Public Health, Fujian Medical University, Fuzhou 350122 Fujian Province, China. ²School of Public Health, Guangzhou Medical University, Guangzhou 511436, China. ³NSW Department of Primary Industries, Wagga Wagga Agricultural Institute, Wagga Wagga, NSW 2650, Australia. ⁴Climate Change Research Centre, University of New South Wales, Sydney, NSW 2052, Australia. ⁵Institute of Health Research, Fujian Medical University, Fuzhou 350122 Fujian Province, China. ⁶These authors contributed equally: Zhi-Ying Zhan, Jun Yang, Xue Zhong. [✉]email: huzhijian@fjmu.edu.cn

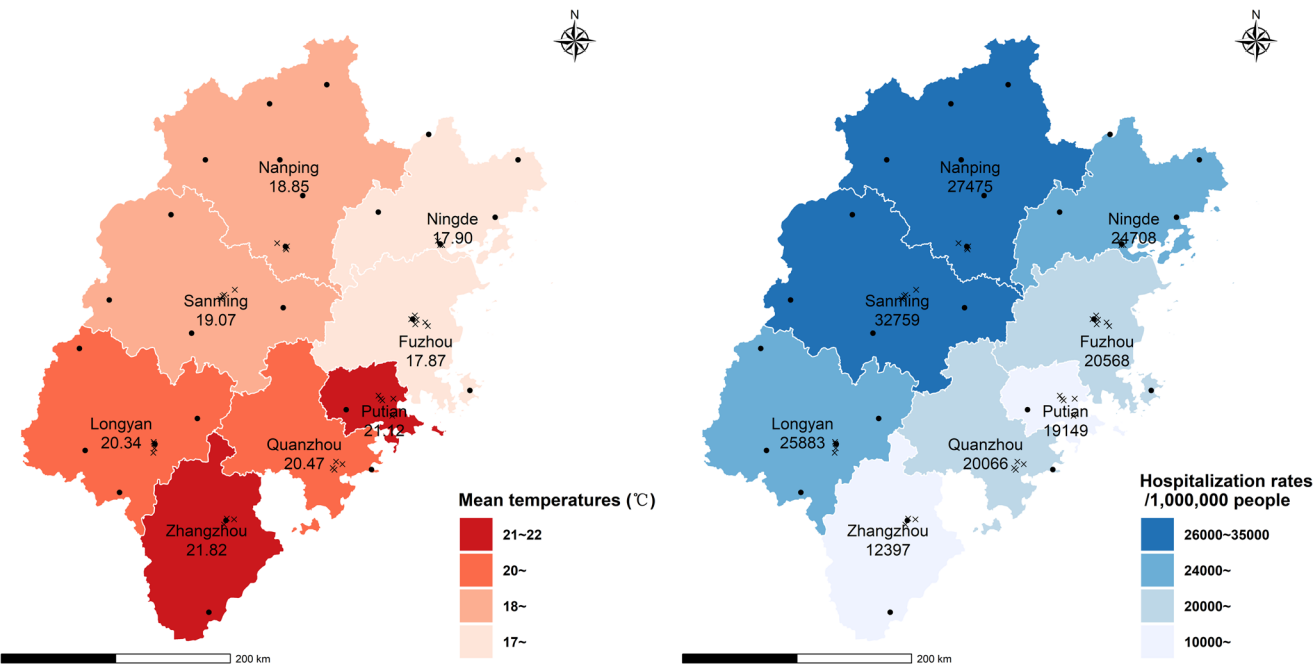


Fig. 1 Annual mean temperature (°C) and hospitalization rate per million population in eight regions in Fujian Province during 2010–2016. The colors represent different ranges of annual mean temperatures (left) and hospitalization rates (right). The dots and the crosses represent weather and air pollution monitoring stations, respectively. Xiamen without hospitalizations of rural residents was excluded.

outcome from future increasing temperature¹⁵. Although climate model projections in Phase 5 of the Coupled Model Intercomparison Project (CMIP5) play an important role in climate research, the CMIP6 have provided multi-model climate projections and added three new emission pathways with the SSP1-2.6, SSP4-3.4 and SSP3-7.0 scenarios to fill the gap between the typical pathways of the CMIP5, which can meet the need of research on impact of future global temperature rises of 1.5 °C and 2.0 °C¹⁶. However, evidence is scarce on projecting health risk of future temperature using the climate models from the Scenario Model Intercomparison Project (ScenarioMIP), a primary activity of the CMIP6.

In this study, we project the excess CVD hospitalizations due to future temperature exposure under four different future climate scenarios. We use hospitalization data for rural population in eight regions in southeastern China and future temperatures projected by 27 general climate models (GCMs); see Supplementary Table 1. We further projected cold-related and heat-related hospitalizations by cause of CVD, individual characteristics, and region. Last, we aimed to estimate the temperature-induced hospitalizations burden of CVD in the future with consideration of both the aging and declining rural population. This study may help identify vulnerable groups, examine effect of the aging and declining rural population, and help develop strategy to prevent potential impacts of future temperature.

RESULTS

There were 2,016,904 CVD hospitalizations recorded from 2010 to 2016 among rural population from the 8 regions in the southern China, and cerebrovascular disease, stroke and ischemic heart disease accounted for 34.84%, 21.47% and 16.85% of the total CVD hospitalizations, respectively. Supplementary Table 2 also shows summary statistics for other environmental factors, and hospitalizations by cause, individual characteristics and regions. Figure 1 shows that the lowest CVD hospitalization rate per million was 12,397 in Zhangzhou, and the highest was 32,759 in Sanming. The lowest averaged daily temperature was 17.87 °C in Fuzhou,

and the highest was 21.82 °C in Zhangzhou during the baseline period.

Figure 2 and Supplementary Figure 1 shows temporal trends of projected temperatures under the four scenarios in Fujian Province and in the eight regions. The projected temperature under the scenarios of SSP3-7.0 and SSP5-8.5 will continue to increase rapidly across the 21st century, while the projected temperature after the middle of this century will slightly increase under the SSP2-4.5 scenario, and will slightly decrease under the SSP1-2.6 scenario. Compared to the baseline period (2010 s), the average temperature will increase by 4.8 °C, 3.7 °C, 2.4 °C and 1.2 °C in 2090 s under the SSP5-8.5, SSP3-7.0, SSP2-4.5 and SSP1-2.6 scenarios, respectively (Supplementary Table 3). The eight regions will have similar absolute temperatures, increasing magnitudes and temperature variability in the 2090 s.

Supplementary Figure 2 shows the baseline temperature–hospitalization associations accumulated over 28 lag days by causes of hospitalization, gender and age groups, with eight region-specific associations in dashed curves. The non-linear temperature–hospitalization associations suggested that both cold and heat increased the hospitalizations risk of CVD. Meanwhile, it was observed that adverse hospitalizations risk attenuated with extremely high temperatures. The minimum hospitalization temperatures was 10.6 °C for cardiovascular disease, similar with subcategories and subgroups.

Table 1 illustrates the future trends of excess hospitalizations attributed to heat and cold by hospitalization causes and individual characteristics under the four scenarios. For the cardiovascular disease, we projected that the fraction of excess hospitalizations attributed to both heat and cold will decrease in the future. The heat-related attributable fraction will decrease from 17.1% (95% eCI: 6.7–25.3) in the 2010 s to 13.4% (95% eCI: -13.0–27.5) in the 2090 s under SSP5-8.5, while the cold-related attributable fraction will decrease from 0.4% to 0.1%. In addition, the temperature-attributable excess CVD hospitalizations will change by 0.1%, -0.7%, -2.5% and -4.0% at the end of the 21st century compared with the 2010 s under all climate scenarios,

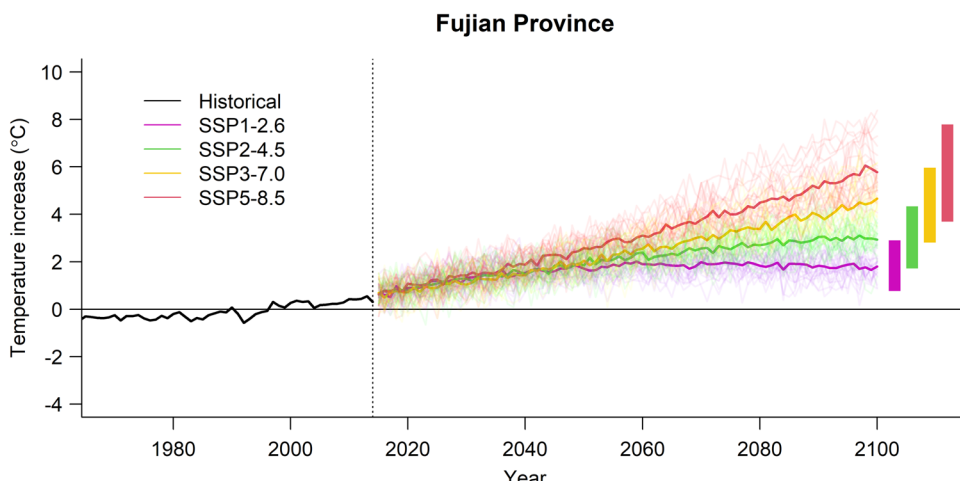


Fig. 2 Temporal trends in projected temperature in Fujian Province. SSP1-2.6, SSP2-4.5, SSP3-7.0 and SSP5-8.5 represent the low, moderate, relative high and high social vulnerability and emission scenarios, respectively. Solid lines denote the mean annual temperature estimated across the 27 general circulation models (GCM), and semi-transparent lines denote GCM-specific temperatures for each year. The four vertical bars on the right show the average annual minimum and maximum for each projected temperature series. Source data are provided in Supplementary Table 3.

respectively, and the change gradients increased in order of SSP1-2.6, SSP2-4.5, SSP3-7.0, and SSP5-8.5 scenarios.

The trends in heat-related hospitalizations varied by subcategories, although there were consistent decreasing trends in cold-related hospitalizations (Table 1). For instance, increasing trends in heat-related hospitalizations are projected for some CVD subcategories, such as ischemic stroke, ischemic heart disease and chronic ischemic heart disease. Compared with in 2010s, the temperature-attributable excess hospitalizations will increase by 1.3–2.0%, 0.6–0.8%, 1.0–2.8%, and 0.1–0.8% in 2090s under four scenarios for ischemic stroke, ischemic heart disease, chronic ischemic heart disease and cerebrovascular disease, respectively. Moreover, the fraction of excess CVD hospitalizations attributable to cold and heat in the future remain higher for the male and the older people than those for the female and the young people. In addition, the trends for cardiovascular disease were similar across regions, but higher heat impacts were observed in Longyan, Ningde and Sanming (Supplementary Table 4).

Table 2 and Supplementary Table 5 shows the cold- and heat-attributable number of excess hospitalizations for different CVD subcategories in the decades of 2050s and 2090s under different combining scenarios of temperature increasing, rural population change and aging. Under no population change scenario, the heat- and cold-attributable number of excess hospitalizations are projected to decrease in the 2090s, except for a slight increase of heat-related hospitalizations under the SSP1. Moreover, the declining rural population will substantially decrease the temperature-related excess CVD hospitalizations in the 2090s under four SSPs, which are 6%, 30%, 65% and 6% of the no population change scenario. Despite the continued decline in the rural population, the population aging will lead to a peak in the number of elderly people in the 2050s and then to a significant increase in heat- and cold-related CVD hospitalizations, which are 2.82, 2.64, 2.34 and 2.87 times higher than those under the four SSPs with only population declining. Similar trends driven by population aging were observed for different subcategories. Population aging will increase the burden of hospitalizations for chronic ischemic heart disease, ischemic stroke, and cerebrovascular disease to a greater degree in the 2050s under the SSP2 and SSP3 scenarios than other subcategories and scenarios, so that the hospitalization burden even exceeds that of the no population decline scenario.

The temperature–hospitalization relationships and the projections of temperature-related hospitalizations were generally robust to variation in the *dfs* ranging from 10 to 12 per year for temporal trends and the *df*s ranging from 4 to 6 for lag days. The projected results remain robust after separately adjusting for environmental factors or excluding PM₁₀ (Supplementary Table 6).

DISCUSSION

This study is to provide evidence on the projections of excess hospitalizations attributable to future temperature from a series of CVD subcategories for rural population in China, using 27 GCMs under four scenarios that emphasize consistency between SSP and RCP. We found that the excess CVD hospitalizations attributable heat and cold generally decrease in future under different scenarios, with the net decrease of 4.0% in hospitalizations attributable to temperature under the SSP5-8.5 scenario in the 2090s compared to the 2010s. For specific subcategories, there were consistent decreasing trends in cold-related hospitalizations, but different trends in heat-related hospitalizations. The net increase in temperature-related hospitalizations are projected to increase with 1.3–2.0% for ischemic stroke under the four scenarios in the 2090s, 0.6–0.8% for ischemic heart disease, 1.0–2.8% for chronic ischemic heart disease, and 0.1–1.0% for cerebrovascular disease. Moreover, future high temperature will cause larger fraction of CVD hospitalizations among male, the elderly and people lived in Longyan and Sanming. Generally, rural population aging will increase the temperature-attributable number of excess CVD hospitalizations in the 2050s, especially under the SSP2 and SSP3 scenarios, and then a dramatic reduction in the size of rural population in the 2090s will reduce the CVD burden attributable to future temperature.

In this study, the excess CVD hospitalizations attributable to cold and heat in rural population are projected to decrease under the majority of future climate change scenarios. Provincially, heat- and cold-related attributable fraction of CVD hospitalizations under the SSP5-8.5 scenario will decrease from 17.1% to 13.4% and from 0.4% to 0.1% respectively during 2010s–2090s. The trends varied slightly across scenarios. However, there was no relevant evidence on projecting the temperature-related excess CVD hospitalizations in rural population. The heat effects at extreme high temperature were mitigated in Fujian, because people tend to stay indoors or in air-conditioned rooms to partly

Table 1. Temperature-related excess hospitalization (%) and 95% empirical confidence intervals indicating the uncertainty by disease, subpopulation, climate change scenario and period.

Disease	Scenario	Effect	2010s	2050s	2090s
Cardiovascular disease	SSP1-2.6	Heat	17.2 (6.7–25.3)	17.4 (5.7–26.3)	17.4 (5.7–26.4)
		Cold	0.4 (−0.1–0.8)	0.2 (−0.1–0.5)	0.2 (−0.1–0.6)
		Net	—	0.0 (−2.2–1.3)	0.1 (−2.4–1.6)
	SSP2-4.5	Heat	17.1 (6.6–25.3)	17.0 (4.9–26.1)	16.7 (3.0–26.7)
		Cold	0.4 (−0.1–0.8)	0.2 (−0.1–0.5)	0.1 (0.0–0.4)
		Net	—	−0.3 (−3.3–1.5)	−0.7 (−6.4–2.4)
	SSP3-7.0	Heat	17.2 (6.7–25.3)	16.7 (4.4–26.0)	15.0 (−4.4–26.8)
		Cold	0.4 (−0.1–0.8)	0.2 (0.0–0.5)	0.1 (0.0–0.2)
		Net	—	−0.6 (−4.3–1.6)	−2.5 (−15.4–3.4)
	SSP5-8.5	Heat	17.1 (6.7–25.3)	16.7 (3.4–26.4)	13.4 (−13.0–27.5)
		Cold	0.4 (−0.1–0.8)	0.1 (0.0–0.3)	0.1 (0.0–0.6)
		Net	—	−0.7 (−5.6–2.1)	−4.0 (−24.9–4.6)
Ischemic heart disease	SSP1-2.6	Heat	20.5 (8.5–30.3)	21.2 (8.8–31.8)	21.3 (8.8–31.9)
		Cold	0.4 (−0.4–1.0)	0.2 (−0.3–0.6)	0.2 (−0.3–0.7)
		Net	—	0.6 (−1.5–2.3)	0.7 (−1.5–2.5)
	SSP2-4.5	Heat	20.5 (8.5–30.3)	21.1 (8.7–31.7)	21.5 (8.2–32.4)
		Cold	0.4 (−0.4–1.0)	0.2 (−0.3–0.6)	0.1 (−0.2–0.4)
		Net	—	0.5 (−2.3–2.7)	0.8 (−4.5–4.6)
	SSP3-7.0	Heat	20.5 (8.4–30.3)	21.0 (8.5–31.6)	21.4 (5.5–32.9)
		Cold	0.4 (−0.4–1.0)	0.2 (−0.3–0.6)	0.1 (−0.1–0.3)
		Net	—	0.4 (−3.0–3.2)	0.6 (−10.8–8.1)
	SSP5-8.5	Heat	20.4 (8.4–30.3)	21.3 (8.3–32.1)	21.4 (0.9–34.6)
		Cold	0.4 (−0.4–1.0)	0.1 (−0.2–0.4)	0.0 (−0.1–0.5)
		Net	—	0.6 (−3.9–4.1)	0.6 (−18.1–11.3)
Chronic ischemic heart disease	SSP1-2.6	Heat	23.8 (12.8–32.5)	24.9 (12.8–34.3)	25.0 (12.9–34.4)
		Cold	0.2 (−0.7–1.0)	0.1 (−0.4–0.6)	0.1 (−0.5–0.7)
		Net	—	1.0 (−1.0–2.7)	1.0 (−0.9–3.0)
	SSP2-4.5	Heat	23.8 (12.7–32.4)	24.9 (12.5–34.4)	25.6 (12.2–35.8)
		Cold	0.2 (−0.7–1.0)	0.1 (−0.4–0.6)	0.0 (−0.3–0.4)
		Net	—	0.9 (−1.5–3.1)	1.6 (−2.7–5.2)
	SSP3-7.0	Heat	23.8 (12.8–32.4)	24.9 (12.3–34.5)	26.1 (10.2–37.4)
		Cold	0.3 (−0.7–1.0)	0.1 (−0.4–0.6)	0.0 (−0.2–0.3)
		Net	—	0.9 (−1.9–3.7)	2.1 (−6.3–8.4)
	SSP5-8.5	Heat	23.8 (12.7–32.4)	25.4 (12.3–35.2)	26.8 (7.5–39.5)
		Cold	0.2 (−0.7–1.0)	0.0 (−0.3–0.4)	0.0 (−0.2–0.3)
		Net	—	1.4 (−2.4–4.6)	2.8 (−10.4–11.4)
Cerebrovascular disease	SSP1-2.6	Heat	22.6 (10.4–31.9)	23.4 (10.2–33.6)	23.5 (10.2–33.7)
		Cold	0.0 (−0.3–0.3)	0.0 (−0.3–0.1)	0.0 (−0.3–0.2)
		Net	—	0.8 (−1.0–2.1)	0.8 (−1.2–2.4)
	SSP2-4.5	Heat	22.5 (10.4–31.9)	23.3 (9.7–33.7)	23.6 (8.6–34.7)
		Cold	0.0 (−0.3–0.3)	0.0 (−0.2–0.1)	0.0 (−0.2–0.1)
		Net	—	0.7 (−1.7–2.4)	1.0 (−3.6–3.8)
	SSP3-7.0	Heat	22.5 (10.4–31.9)	23.2 (9.3–33.7)	23.1 (4.5–35.7)
		Cold	0.0 (−0.3–0.3)	0.0 (−0.3–0.1)	0.0 (−0.2–0.1)
		Net	—	0.6 (−2.3–2.6)	0.5 (−9.2–5.2)
	SSP5-8.5	Heat	22.5 (10.4–31.9)	23.5 (8.9–34.4)	22.6 (−1.2–37.0)
		Cold	0.0 (−0.3–0.3)	0.0 (−0.2–0.1)	0.0 (−0.1–0.1)
		Net	—	0.9 (−3.1–3.3)	0.1 (−15.5–6.8)
Stroke	SSP1-2.6	Heat	12.3 (−6.9–26.8)	12.7 (−10.7–29.2)	12.7 (−10.7–29.3)
		Cold	0.3 (−0.4–0.8)	0.1 (−0.2–0.4)	0.2 (−0.2–0.6)
		Net	—	0.3 (−4.3–2.7)	0.4 (−4.4–2.9)

Table 1 continued

Disease	Scenario	Effect	2010s	2050s	2090s
Ischemic stroke	SSP2-4.5	Heat	12.2 (-7.1–26.8)	12.6 (-12.4–29.6)	12.6 (-17.3–31.7)
		Cold	0.3 (-0.4–0.8)	0.1 (-0.2–0.5)	0.1 (-0.1–0.3)
		Net	—	0.2 (-6.0–3.2)	0.2 (-11.8–5.3)
	SSP3-7.0	Heat	12.2 (-6.9–26.7)	12.4 (-13.8–30.0)	11.6 (-29.8–33.9)
		Cold	0.3 (-0.4–0.8)	0.1 (-0.2–0.5)	0.1 (-0.1–0.2)
		Net	—	0.1 (-7.5–3.7)	-0.8 (-26.2–8.0)
	SSP5-8.5	Heat	12.2 (-7.1–26.8)	12.5 (-16.0–31.1)	10.5 (-47.9–36.0)
		Cold	0.3 (-0.4–0.8)	0.1 (-0.1–0.3)	0.1 (0.0–0.3)
		Net	—	0.1 (-10.1–4.6)	-2.0 (-44.8–10.4)
	SSP1-2.6	Heat	21.8 (5.5–33.7)	23.2 (3.3–36.8)	23.2 (3.2–36.8)
		Cold	0.2 (-0.4–0.8)	0.1 (-0.2–0.4)	0.1 (-0.2–0.5)
		Net	—	1.3 (-2.9–3.5)	1.3 (-3.1–3.9)
	SSP2-4.5	Heat	21.8 (5.3–33.8)	23.3 (1.9–37.3)	24.0 (-2.5–39.8)
		Cold	0.2 (-0.4–0.8)	0.1 (-0.2–0.5)	0.1 (-0.2–0.3)
		Net	—	1.3 (-4.5–4.1)	2.0 (-9.7–7.1)
	SSP3-7.0	Heat	21.8 (5.5–33.7)	23.3 (0.8–37.8)	24.0 (-16.9–43.6)
		Cold	0.3 (-0.4–0.8)	0.1 (-0.2–0.5)	0.0 (-0.1–0.2)
		Net	—	1.3 (-5.9–5.0)	2.0 (-25.6–11.1)
	SSP5-8.5	Heat	21.8 (5.4–33.7)	23.7 (-1.4–39.1)	23.6 (-38.4–46.8)
		Cold	0.2 (-0.4–0.8)	0.1 (-0.2–0.3)	0.0 (-0.1–0.3)
		Net	—	1.8 (-8.3–6.2)	1.6 (-48.2–14.8)
Male	SSP1-2.6	Heat	21.9 (12.4–30.4)	22.7 (11.6–32.4)	22.8 (11.6–32.5)
		Cold	0.6 (0.0–1.1)	0.3 (0.0–0.7)	0.4 (0.0–0.9)
		Net	—	0.5 (-1.2–2.0)	0.6 (-1.3–2.3)
	SSP2-4.5	Heat	21.9 (12.3–30.4)	22.5 (10.9–32.5)	22.6 (9.2–33.8)
		Cold	0.7 (0.0–1.1)	0.3 (0.0–0.8)	0.2 (0.0–0.6)
		Net	—	0.3 (-1.9–2.2)	0.3 (-3.9–3.4)
	SSP3-7.0	Heat	21.9 (12.4–30.3)	22.3 (10.3–32.6)	21.5 (4.3–34.8)
		Cold	0.7 (0.0–1.2)	0.4 (0.0–0.7)	0.2 (0.0–0.4)
		Net	—	0.1 (-2.5–2.3)	-0.9 (-10.1–4.3)
	SSP5-8.5	Heat	21.8 (12.3–30.3)	22.5 (9.7–33.3)	20.4 (-1.8–36.0)
		Cold	0.7 (0.0–1.1)	0.2 (0.0–0.5)	0.1 (0.0–0.9)
		Net	—	0.3 (-3.4–2.9)	-1.9 (-16.5–5.7)
Female	SSP1-2.6	Heat	13.0 (-0.5–24.1)	12.8 (-2.2–24.7)	12.8 (-2.1–24.8)
		Cold	0.2 (-0.5–0.7)	0.1 (-0.3–0.4)	0.1 (-0.3–0.5)
		Net	—	-0.3 (-3.7–2.0)	-0.2 (-3.8–2.1)
	SSP2-4.5	Heat	12.9 (-0.6–24.1)	12.4 (-2.9–24.6)	11.8 (-5.6–25.3)
		Cold	0.2 (-0.5–0.7)	0.1 (-0.3–0.4)	0.0 (-0.2–0.3)
		Net	—	-0.7 (-5.1–2.4)	-1.3 (-9.9–4.1)
	SSP3-7.0	Heat	13.0 (-0.6–24.0)	12.1 (-3.7–24.5)	9.9 (-14.8–26.1)
		Cold	0.2 (-0.5–0.7)	0.1 (-0.3–0.4)	0.0 (-0.2–0.2)
		Net	—	-1.0 (-6.5–2.8)	-3.2 (-22.7–7.0)
	SSP5-8.5	Heat	12.9 (-0.6–24.0)	11.9 (-4.9–24.9)	8.0 (-28.0–27.5)
		Cold	0.2 (-0.5–0.7)	0.0 (-0.2–0.3)	0.0 (-0.1–0.2)
		Net	—	-1.2 (-8.6–3.6)	-5.1 (-37.0–9.7)
Age, 0–64 years	SSP1-2.6	Heat	12.3 (-5.2–26.0)	11.8 (-7.9–27.3)	11.9 (-7.9–27.4)
		Cold	0.4 (-0.3–1.0)	0.2 (-0.2–0.6)	0.2 (-0.2–0.7)
		Net	—	-0.6 (-3.6–1.4)	-0.5 (-3.8–1.6)
	SSP2-4.5	Heat	12.2 (-5.3–26.0)	11.4 (-9.2–27.3)	10.6 (-12.6–28.3)
		Cold	0.4 (-0.3–1.0)	0.2 (-0.2–0.7)	0.1 (-0.2–0.5)
		Net	—	-1.1 (-4.9–1.5)	-1.9 (-9.0–2.5)
	SSP3-7.0	Heat	12.2 (-5.2–26.0)	11.0 (-10.1–27.4)	8.3 (-21.2–29.1)
		Cold	0.4 (-0.3–1.1)	0.2 (-0.2–0.7)	0.1 (-0.1–0.3)

Table 1 continued

Disease	Scenario	Effect	2010s	2050s	2090s
Age, 65–74 years	SSP5-8.5	Net	—	−1.5 (−6.0–1.6)	−4.3 (−19.3–3.7)
		Heat	12.2 (−5.3–26.0)	10.7 (−11.8–27.8)	6.2 (−31.4–30.5)
		Cold	0.4 (−0.3–1.0)	0.1 (−0.2–0.5)	0.1 (−0.1–0.6)
	SSP1-2.6	Net	—	−1.8 (−8.0–2.1)	−6.4 (−30.6–5.2)
		Heat	22.5 (13.5–29.8)	23.6 (13.9–31.5)	23.6 (14.0–31.6)
		Cold	0.3 (−0.6–1.0)	0.1 (−0.4–0.6)	0.2 (−0.4–0.7)
	SSP2-4.5	Net	—	0.9 (−0.7–2.4)	1.0 (−0.7–2.7)
		Heat	22.5 (13.5–29.9)	23.5 (13.9–31.6)	24.1 (14.0–32.6)
		Cold	0.3 (−0.6–1.1)	0.1 (−0.4–0.6)	0.1 (−0.3–0.4)
	SSP3-7.0	Net	—	0.8 (−1.3–2.8)	1.4 (−2.4–4.5)
		Heat	22.5 (13.4–29.8)	23.5 (13.8–31.6)	24.2 (12.3–33.7)
		Cold	0.3 (−0.6–1.1)	0.1 (−0.4–0.6)	0.0 (−0.2–0.3)
Age, ≥75 years	SSP5-8.5	Net	—	0.8 (−1.7–3.2)	1.4 (−6.2–7.1)
		Heat	22.5 (13.4–29.8)	23.9 (14.0–32.2)	24.4 (9.6–35.3)
		Cold	0.3 (−0.6–1.0)	0.1 (−0.3–0.4)	0.0 (−0.1–0.4)
	SSP1-2.6	Net	—	1.2 (−2.1–4.0)	1.7 (−10.5–9.8)
		Heat	18.2 (2.8–30.5)	18.5 (0.8–32.4)	18.6 (0.9–32.5)
		Cold	0.6 (0.0–1.1)	0.3 (0.0–0.7)	0.4 (0.0–0.9)
	SSP2-4.5	Net	—	−0.0 (−3.2–2.2)	0.1 (−3.4–2.4)
		Heat	18.2 (2.7–30.5)	18.2 (−0.3–32.6)	17.7 (−4.4–33.9)
		Cold	0.6 (0.0–1.1)	0.3 (0.0–0.8)	0.2 (0.0–0.6)
	SSP3-7.0	Net	—	−0.3 (−4.7–2.5)	−0.9 (−9.3–4.0)
		Heat	18.2 (2.8–30.5)	17.8 (−1.3–32.6)	15.4 (−14.5–35.0)
		Cold	0.6 (0.0–1.2)	0.3 (0.0–0.7)	0.2 (0.0–0.4)
	SSP5-8.5	Net	—	−0.7 (−6.0–2.7)	−3.3 (−21.5–5.7)
		Heat	18.2 (2.8–30.5)	17.8 (−3.0–33.5)	13.2 (−27.4–36.6)
		Cold	0.6 (0.0–1.1)	0.2 (0.0–0.5)	0.1 (0.0–0.8)
		Net	—	−0.8 (−8.0–3.5)	−5.6 (−35.8–7.8)

mitigate heat effects during extremely hot days, which resulted in the decreasing trend projected for heat-related excess hospitalizations from CVD under global warming. This finding underscores the importance of policy and measurement improving population adaptation to global warming. Previous studies have found heat will increase mortality due to CVD under climate change, while cold will decrease the burden^{7,8}, and similar trends were reported on years of life lost (YLL) and out-of-hospital cardiac arrest^{10,17}. However, it is still inconsistent that whether the cold-related decreasing trend can offset the heat-related increasing trend in mortality and YLL. Thus, the CVD health outcome (morbidity and mortality) related to future cold and heat need to be confirmed in more research.

We found that both the declining and aging rural population in the future may substantially affect the burden of CVD hospitalizations associated with future rising temperatures. The declining rural population would substantially decrease the temperature-related CVD hospitalizations. It may be the reason that rapid urbanization will monotonically and substantially decrease the rural population size under the four SSPs in the Fujian Province. Although a substantial reduction in the total rural population will attenuate the projected excess CVD hospitalizations related to future temperature in rural regions, the rural population aging will still elevate temperature-related CVD hospitalizations in the 2050s that is 2.82, 2.64, 2.34 and 2.87 times under four SSPs with population declining and aging compared to those with only population declining. Yang and co-authors found similar results that the population aging is detected to rapidly rise the excess

mortality related to heat in the northeastern region in China, which is probably associated with both high population out-migration and long life expectancy^{7,18}. With the serious challenges of an aging population, our findings may be beneficial in the improvement of relevant health care planning and public health activities to counteract the future cold and heat to protect the elderly.

Increasing trends in heat-related hospitalizations is projected for ischemic heart disease, cerebrovascular and ischemic stroke. Due to different physiological mechanisms, the shapes of the temperature–hospitalization association varied by subcategories, which might lead to inconsistencies in the predicted hospitalizations burden from different CVD subcategories related to temperature. Previous studies confirmed that future high temperature is likely to increase mortality from ischemic heart disease and cerebrovascular disease from the 2010s to 2090s in Ningbo, China¹⁹, and to increase mortality from acute ischemic heart disease and ischemic stroke from the decades of 1980s to 2080s under RCP4.5 and RCP8.5 scenarios¹¹. The projected number of excess hospitalizations from cerebrovascular disease associated with heat is greater than those from other subcategories in our study, with at least 226,776 excess hospitalizations in the 2090s under scenarios, which is probably associated with higher hospitalization rate. Thus, continuous attention and epidemic surveillance to the disease is necessary to reduce the health burden.

We found the elderly and males were more susceptible to the future climate change than the young and female. The poorer

Table 2. Temperature-related number of CVD hospitalizations in 2010s, 2050s and 2090s, under different combining scenarios of temperature increasing, population change, and population aging.

Temperature scenario	Population change	Population aging	Heat			Cold		
			2010s	2050s	2090s	2010s	2050s	2090s
SSP1-2.6	No change	No change	494928	500173	502412	11349	5540	6548
SSP1-2.6	SSP1	No change	494928	199349	26365	11349	1923	205
SSP1-2.6	SSP1	SSP1	475700	563030	86779	12785	7058	1225
SSP2-4.5	No change	No change	493719	490821	481480	11553	5501	3422
SSP2-4.5	SSP2	No change	493719	290146	142273	11553	3044	888
SSP2-4.5	SSP2	SSP2	474485	765241	401259	12999	9954	3771
SSP3-7.0	No change	No change	494295	482368	432198	11885	5811	2180
SSP3-7.0	SSP3	No change	494295	403186	279852	11885	4697	1310
SSP3-7.0	SSP3	SSP3	475034	941840	603960	13358	12719	3848
SSP5-8.5	No change	No change	493461	481561	387360	11465	3730	1711
SSP5-8.5	SSP5	No change	493461	193752	21395	11465	1259	26
SSP5-8.5	SSP5	SSP5	474225	556178	66823	12912	4944	296

cardiorespiratory and circulatory conditions of the majority of the elderly may weaken their thermoregulatory capacity and increase their vulnerability. Limited evidence on vulnerable population to the future temperature effect on CVD hospitalizations is available for the rural population. Previous studies reported, in rural population, the effect modification of temperature on hospitalizations from CVD diseases by age and gender were inconsistent in western and southeastern suburbs in China^{6,20}. We also found spatial heterogeneity in future temperature impact on CVD hospitalizations. The fraction attributable to future temperature was higher in Longyan, Ningde and Sanming regions, with relatively lower socioeconomic status. Previous studies also reported that the poverty exacerbated the cold- and heat-related cardiorespiratory mortality²¹ and hospitalizations⁶. However, the existing evidence on effect modification were based on historical data, and more research is need to provide relevant evidence of future temperature impact on CVD hospitalizations.

The changes in hospitalizations attributable to future temperature varied across different climate scenarios, which is similar to existing evidence on mortality⁷. For all causes, the slopes of changes are steeper under SSP5-8.5 scenario. Notably, although the future risks seem reduce for some subcategories under SSP5-8.5, it is not yet possible to draw conclusions about the impact of increasing temperature on public health. Limited evidence on projection of temperature-related excess CVD hospitalizations is available from different regions with various climate to confirm the conclusion, especially in rural population. In addition, a study conducted in 451 locations in countries worldwide projected that the excess mortality related to temperature will increase on average under high-emission scenarios, although with an apparent heterogeneity across locations¹⁴.

This study estimates the future temperature-related excess CVD hospitalizations accounting for uncertainties from 27 climate models, four emission scenarios, future aging and declining rural population, and imprecision of the estimated association. However, additional sources of uncertainties still deserve attention, including population structure changes, population adaptation and acclimatization. The findings in this study should be considered as potential effects of future temperatures on CVD hospitalizations under hypothetical scenarios, because we assumed the shape of the temperature–hospitalizations curve to be unchanged at the level of the 2010s throughout the study period, ignoring the potential changes in climate adaptive capability. However, the extent of population adaptation is still unclear. Moreover, this study did not consider population

acclimatization to increasing temperatures, which might overestimate the risk of future temperatures on CVD hospitalizations. However, there is limited and inconsistent evidence regarding influence of population acclimatization on health risk^{7,22}. In addition, although this study has accounted for population structure by using age-specific risks, potential changes in disease spectrum and demographic characteristics (e.g., educational attainment and social position) may modify the vulnerability of population to future temperature, by increasing the population at risk or with higher risks. Future study is needed to properly account for these sources of uncertainty when assessing health burden related to future temperature.

This study had some limitations. First, similar to many previous studies, baseline temperature from fixed monitoring sites cannot adequately reflect individual exposure, although these measurement errors are probably distributed randomly. Second, the current SSP scenarios cannot fully represent the region-specific ratio of the elderly and population size, which probably result in a conservative estimate of excess CVD hospitalizations related to future temperature. More studies are needed to quantify future population changes at a finer scale more accurately. Third, we assumed the disease spectrum remains constant according to the previous study^{7,19}, which may underestimate the projections of CVD hospitalizations. The increasing trends of global elderly and obese population²³ will increase the number of high-risk population. Moreover, temperature increased risks in almost all subcategories⁶, and changes in disease spectrum probably increase the small subcategories with higher temperature effects. Fourth, it should be cautious to generalize these finding to other regions, especially regions with different climatic conditions, degree of urbanization, and population change. Finally, although the analyzed dataset could not identify whether the hospitalizations were planned in advance or not, the impact of pre-planned hospitalizations on the results is limited, because the Chinese rural population generally lacked awareness of cardiovascular disease health management during the studied period²⁴.

METHODS

Study population and region

This study was carried out in eight regions along the Chinese southeastern coast, including Fuzhou, Longyan, Nanping, Ningde, Putian, Quanzhou, Sanming and Zhangzhou regions, where a subtropical marine monsoon climate characterized by long-lasting

high temperatures in summer prevails. The detailed information have been described in our previous study⁶.

Data collection

We have collected the data of hospitalizations and temperature during the baseline period. Records of individual hospitalizations for rural population in the regions during 2010–2016 were collected from the New Rural Cooperative Medical Scheme that had covered >85% of the rural population since 2007²⁵. Based on the tenth version of the International Classification of Diseases (ICD-10), we selected and categorized the hospitalization records into the total cardiovascular diseases (I00–I99) and five subcategories with sufficient occurrences (Supplementary Table 2). We have aggregated the total number of CVD hospitalizations per day, broken down by cause of hospitalizations, age groups (0–64, 65–74, and ≥75 years old) and gender groups. The rates of extreme outliers exceeding the median by above three times the interquartile range were <0.22% for the analyzed variables, which were replaced by the average of counts from two adjacent days. We also collected the daily weather (temperature and relative humidity) from the China Meteorological Data Service Center, and air pollution data (particulate matter with diameters below 10 µm, nitrogen dioxide and sulfur dioxide) from the China National Environmental Monitoring Centre during the baseline period. All variables had no missing values except for PM₁₀ concentration with a low missing rate of 2.38%, and the missing values were not processed. The detailed information is shown in Supplementary Table 2 and our previous study⁶.

The ScenarioMIP design is the primary activity within the project of CMIP6 that provides multi-model climate projections based on various scenarios related to societal concerns of climate change mitigation, adaptation, or impacts²⁶. It has projected future temperatures from 1961 to 2100 considering land use and greenhouse gas concentrations. We acquired downscaled future temperature projections under the core test, including 4 scenarios and using 27 general circulation models. These scenarios (i.e., SSPx-y) have indicated that adopting climate adaptation and mitigation policies under specific Shared Socioeconomic Pathways (SSPs, x) will lead to the corresponding outcome of the Representative Concentration Pathways (RCPs, y)²⁷. The SSP1-2.6 scenario indicates a combination of low social vulnerability and a radiative forcing of 2.6 W/m², with a temperature rise below 2°C in 2100, which can support the environment-related research on the target of 2 °C temperature rise. The SSP2-4.5, SSP3-7.0 and SSP5-8.5 scenarios illustrate moderate, relatively high, and high social vulnerability and radiative forcing of 4.5 W/m², 7.0 W/m² and 8.5 W/m², of which temperature will rise about 3.07 °C, 4.06 °C and 5.17 °C by 2100, respectively²⁸. In addition, we downscaled the monthly gridded data of GCMs to daily scale for the regions in this study, using the statistical downscaling model NWAI-WG²⁹. First, spatial downscaling involved an inverse distance-weighted interpolation based on the center of the nearest four grid points in the GCMs. Second, bias correction of the GCM-projected monthly values and historically observed temperatures was performed using an equidistant quantile method. Finally, the daily time series of temperature were downscaled from the bias-corrected monthly GCM projections using a modified version of a stochastic weather generator³⁰. To date, the NWAI-WG downscaled data have been used in many previous studies on health risk assessment of climate change^{7,31–34}.

We collected the gridded rural population projections for the eight regions from 2010 to 2099 from the database of spatial population scenario as a published study⁷. The population of 1 km × 1 km grid cells within each region were summed up to obtain the projected region-specific and SSP-specific rural population, which were further adjusted by the region-specific correction factors that were assumed to be constant and calculated by

comparing the 2010 projected population from the SSPs to the 2010 population census. We selected the four future population growth scenarios including SSP1, SSP2, SSP3, and SSP5, corresponding to the above future climate scenarios, representing different levels of fertility, migration, education, and mortality³⁵. A no population change scenario was also considered as a reference group. The rural population continued to influx into cities due to continuous urbanization, especially the young people, so that the size of rural population will monotonically decrease in future different from the whole population, leading to the smallest rural population of 7459 in Ningde under the SSP1 with low birth rate and moderate migration rate (Supplementary Figure. 3). Thus, to account for the effects of dramatic changes in the rural population size and structure, we projected region-specific rural population size for the age groups during 2010–2099¹⁸. Consistent with the published study⁷, the provincial proportions between age groups were used for the local municipal regions due to data availability. Future rural population in the eight regions in southeastern China by age groups is presented (Supplementary Figure. 3). The population aging will increase the number of elderly people, especially in the region with large total population. The future population size will decrease more slowly under the SSP3 with high fertility rate and low migration rate than under other scenarios, especially in Quanzhou which has a large population base and developed commerce.

Statistical analysis

Firstly, we established the temperature–hospitalization relationship using a conventional two-stage method based on the baseline data from 2010 to 2016. Secondly, combining the established relationship, modeled temperature and hospitalizations projections, we projected the daily number of hospitalizations caused by temperature for each day between 2010 and 2099. Lastly, we considered the influence of changes in the rural population on the anticipated burden related to temperature in the future. Details of each step are provided below.

The traditional two-stage analyses were employed to estimate the baseline association of hospitalizations due to various causes with historical temperature. First, a quasi-Poisson model was used to fit region-specific temperature–hospitalization relationships allowing the overdispersion of count data, combined with distributed lag non-linear model (DLNM) taking the nonlinear temperature effect over lag days into consideration³⁶. The model was specified follows:

$$\log E[Y_t] = \alpha + \beta Temp_{t,l} + ns(Time_t, 12 \times 7) + ns(PM10_t, 3) + DOW_t + Holiday_t \quad (1)$$

where t is the day of observation, Y_t and $E(Y_t)$ are the observed and expected counts of daily hospitalizations, respectively. The DLNM generated a two-dimensional cross-basis function for temperature ($Temp_{t,l}$) consisted of a natural cubic spline function (ns) with three knots at the 10th, 50th and 90th percentiles of temperature to estimate a nonlinear temperature–hospitalization relationship³⁷, and a ns function with three knots at equally log-scale spaced values of 28 lag days to estimate nonlinear lag–hospitalization relationship. The ns allows the log-linear extrapolation of the function beyond the range of the monitored temperature series, which is required to project hospitalization risk of future temperatures³⁸. The model also controlled for the confounding effects of long-term trends and seasonality using a ns of $Time_t$ with 12 degrees of freedom (df) per year, $PM10_t$ using a ns of $PM10_t$ with 3 df , day of the week (DOW_t) and public holidays. The choice of parameters for the core model depended on the best-fitting model, with the minimum Akaike's information criterion that is commonly used to compare possible models (Supplementary Table 7). We selected the reference of the minimum hospitalization temperature (MHT) of the temperature–hospitalization

association accumulated over lag days. α and β are the coefficients. Second, the region-specific relationships were pooled together through a multivariate meta-analysis using restricted maximum likelihood^{37,39}. Then, to ensure the stability, the region-specific cumulative relationships between temperature and hospitalizations re-estimated by the best linear unbiased prediction (BLUP). The BLUP estimated the region-specific associations by combining the region-specific and the average parameters with weights inversely proportional to their variability, which could provide precise estimations in regions with small number of events. This methodology has been described in detail in previous studies^{39,40}.

Briefly, based on modeled temperature, hospitalizations projections and the established temperature–hospitalization relationship, we computed the daily amount of hospitalizations due to temperature for any baseline and future days. Cold days and hot days were defined according to daily temperatures below and above the MHT respectively, and collectively referred to as non-optimal temperature days. The sum of the excess hospitalizations for all cold days and all hot days are the number of hospitalizations attributed to cold and heat respectively, and the sum of both is the number of hospitalizations attributed to non-optimal temperatures. The fraction of the number of hospitalizations attributed to non-optimal temperature (i.e., cold and heat) to the total number of hospitalizations was the attributable fraction (AF). The modeling framework has been elaborated in a recently published paper³⁸, and has been adopted in other studies^{7,19}. We separately estimated decadal heat- and cold-related excess CVD hospitalizations by different regions, SSPs and GCMs. The attributable fractions were computed for different regions, decade and SSP through dividing the GCM-ensemble averages by the corresponding total number of hospitalizations. The uncertainties of the projections of hospitalizations attributed to heat and cold are mainly caused by the estimated exposure-response relationships and projected temperature among different GCMs. To quantify these uncertainties, we computed the 2.5th and 97.5th percentiles of the results for combinations of 27 GCMs and 1000 simulated samples of reduced BLUP coefficients as the 95% empirical confidence intervals (eCI), using the Monte Carlo simulation assuming a multivariate normal distribution for coefficients of spline model³⁸.

Considering the impact of rural population change on future temperature-related burden is essential due to sharp declines in rural population size and increasing proportions of elderly populations in the future. First, temperature–hospitalization associations were estimated for different age groups using the time-series analysis described above. Then, the number of hospitalizations attributed to future temperature for each age group was projected based on the age-specific baseline associations and age-specific future population change ratio comparing to the decade of 2010 under four SSP scenarios.

We projected future temperature-related excess hospitalizations by causes, regions, age groups, gender groups to identify the susceptible populations in future. The excess hospitalizations attributed to heat and cold under different climate change scenarios were provided for the decades of 2010s from 2010 to 2019, 2050s from 2050 to 2059 and 2090s from 2090 to 2099.

In addition, we performed a series of sensitivity analyses to test robustness of the main results. The df is an important parameter in a natural cubic spline to determine the number of intervals dividing the domain of independent variables, and a third-order polynomial is used to fit nonlinear association in each interval. We selected the appropriate dfs from those commonly used (Supplementary Table 7) that could consider the temporal trend and lagged effects sufficiently. To consider the influence, we further conducted a common practice using alternative dfs adjacent to the selected, including dfs of 10 and 11 per year for

time trends, and alternative dfs of 4 and 6 for maximum lag days, respectively. The main model excluded the PM_{10} to consider the influence of missing values, although the missing rate was low. In addition, the main model also separately added the ns with 3 df of other environmental factors, such as rainfall (mm), sunshine duration (hours), NO_2 ($\mu\text{g}/\text{m}^3$) and SO_2 ($\mu\text{g}/\text{m}^3$). The software of R with version number 4.0.5 were used to implement all statistical analyses.

Ethics statement

This study has been approved by the Ethics Committee of the Fujian Medical University (No. 202182). No participants were contacted, and data were analyzed at an aggregate level.

DATA AVAILABILITY

Data are publicly available from the websites for baseline weather data (<http://data.cma.cn/>), baseline air pollution data (<http://www.cnemc.cn/>), projected population (<https://www.cgd.ucar.edu/sections/iam/modeling/spatial-population>) and projected temperatures (<https://esgf-node.llnl.gov/search/cmip6/>). Raw data of hospitalizations were collected under a data sharing agreement, and the authors are not authorized to redistribute the data.

CODE AVAILABILITY

The code is available upon request.

Received: 31 December 2022; Accepted: 24 July 2023;
Published online: 05 August 2023

REFERENCES

1. World Health Organization. Cardiovascular Diseases (CVDs). [https://www.who.int/news-room/fact-sheets/detail/cardiovascular-diseases-\(cvds\)](https://www.who.int/news-room/fact-sheets/detail/cardiovascular-diseases-(cvds)) (2021).
2. Lozano, R. et al. Global and regional mortality from 235 causes of death for 20 age groups in 1990 and 2010: a systematic analysis for the Global Burden of Disease Study 2010. *Lancet* **380**, 2095–2128 (2012).
3. Dagenais, G. R. et al. Variations in common diseases, hospital admissions, and deaths in middle-aged adults in 21 countries from five continents (PURE): a prospective cohort study. *Lancet* **395**, 785–794 (2020).
4. National Center for Cardiovascular Diseases. *Report on Cardiovascular Diseases in China 2018* Vol. 1 (Encyclopedia of China Publishing House, 2018).
5. IPCC. *Summary for Policymakers. Climate Change 2022: Impacts, Adaptation and Vulnerability. Contribution of Working Group II to the Sixth Assessment Report of the Intergovernmental Panel on Climate Change.* (Cambridge University Press, Cambridge, UK and New York, NY, USA, 2022).
6. Zhan, Z. et al. Effect of apparent temperature on hospitalization from a spectrum of cardiovascular diseases in rural residents in Fujian, China. *Environ. Pollut.* **303**, 119101 (2022).
7. Yang, J. et al. Projecting heat-related excess mortality under climate change scenarios in China. *Nat. Commun.* **12**, 1039 (2021).
8. Zhang, B., Li, G., Ma, Y. & Pan, X. Projection of temperature-related mortality due to cardiovascular disease in Beijing under different climate change, population, and adaptation scenarios. *Environ. Res.* **162**, 152–159 (2018).
9. Cai, W. et al. The 2021 China report of the Lancet Countdown on health and climate change: seizing the window of opportunity. *Lancet Public Health* **6**, e932–e947 (2021).
10. Li, G., Li, Y., Tian, L., Guo, Q. & Pan, X. Future temperature-related years of life lost projections for cardiovascular disease in Tianjin, China. *Sci. Total Environ.* **630**, 943–950 (2018).
11. Li, T. et al. Long-term projections of temperature-related mortality risks for ischemic stroke, hemorrhagic stroke, and acute ischemic heart disease under changing climate in Beijing, China. *Environ. Int.* **112**, 1–9 (2018).
12. Li, Y., Ren, T., Kinney, P. L., Joyner, A. & Zhang, W. Projecting future climate change impacts on heat-related mortality in large urban areas in China. *Environ. Res.* **163**, 171–185 (2018).
13. United Nations. *World Population Ageing 2017: Highlights* (United Nations New York, 2017).
14. Gasparri, A. et al. Projections of temperature-related excess mortality under climate change scenarios. *Lancet Planet. Health* **1**, e360–e367 (2017).

15. Sanderson, M., Arbuthnott, K., Kovats, S., Hajat, S. & Falloon, P. The use of climate information to estimate future mortality from high ambient temperature: a systematic literature review. *Plos One* **12**, e180369 (2017).
16. Zhang, L. X., Chen, X. L. & Xin, X. G. Short commentary on CMIP6 scenario model Intercomparison project (ScenarioMIP). *Clim. Chang. Res.* **15**, 519–525 (2019).
17. Onozuka, D., Gasparrini, A., Sera, F., Hashizume, M. & Honda, Y. Future projections of temperature-related excess out-of-hospital cardiac arrest under climate change scenarios in Japan. *Sci. Total Environ.* **682**, 333–339 (2019).
18. Jiang, T. et al. National and provincial population projected to 2100 under the shared socioeconomic pathways in China. *Clim. Chang. Res.* **13**, 128–137 (2017).
19. Gu, S. et al. Projections of temperature-related cause-specific mortality under climate change scenarios in a coastal city of China. *Environ. Int.* **143**, 105889 (2020).
20. Wang, B. et al. Impact of ambient temperature on cardiovascular disease hospital admissions in farmers in China's Western suburbs. *Sci. Total Environ.* **761**, 143254 (2021).
21. Zhang, Y. et al. Socio-geographic disparity in cardiorespiratory mortality burden attributable to ambient temperature in the United States. *Environ. Sci. Pollut. R.* **26**, 694–705 (2019).
22. Baccini, M. et al. Impact of heat on mortality in 15 European cities: attributable deaths under different weather scenarios. *J. Epidemiol. Commun. H.* **65**, 64–70 (2011).
23. World Obesity Federation. *World Obesity Atlas* 2023. https://www.worldobesityday.org/assets/downloads/World_Obesity_Atlas_2023_Report.pdf (2023).
24. Ma, L. Y. et al. China cardiovascular diseases report 2018: an updated summary. *J. Geriatr. Cardiol.* **17**, 1–8 (2020).
25. Fujian Health and Family Planning Commission. *The Achievements of the "Twelfth Five-Year Plan" in Health Service of Fujian Province*. https://wjw.fujian.gov.cn/xxgk/zfxxgkzl/zfxxgkml/ghjh/201603/t20160317_2372761.htm (2016).
26. O'Neill, B. C. et al. The Scenario Model Intercomparison Project (ScenarioMIP) for CMIP6. *Geosci. Model Dev.* **9**, 3461–3482 (2016).
27. Kriegler, E. et al. The need for and use of socio-economic scenarios for climate change analysis: a new approach based on shared socio-economic pathways. *Global Environ. Chang.* **22**, 807–822 (2012).
28. Zhao, S. et al. Datasets for the CMIP6 Scenario Model Intercomparison Project (ScenarioMIP) Simulations with the coupled model CAS FGOALS-f3-L. *Adv. Atmos. Sci.* **38**, 329–339 (2021).
29. Liu, D. & Zuo, H. Statistical downscaling of daily climate variables for climate change impact assessment over New South Wales, Australia. *Clim. Change* **115**, 629–666 (2012).
30. Richardson C. W., Wright D. A. *WGGEN: A Model for Generating Daily Weather Variables*. (U.S. Department of Agriculture, Agricultural Research Service, 1984).
31. Guo, Y. et al. Projecting future temperature-related mortality in three largest Australian cities. *Environ. Pollut.* **208**, 66–73 (2016).
32. Hundessa, S. et al. Projecting potential spatial and temporal changes in the distribution of Plasmodium vivax and Plasmodium falciparum malaria in China with climate change. *Sci. Total Environ.* **627**, 1285–1293 (2018).
33. Zhao, Q. et al. Modeling the present and future incidence of pediatric hand, foot, and mouth disease associated with ambient temperature in mainland China. *Environ. Health Persp.* **126**, 47010 (2018).
34. Liu, J. et al. Projecting the excess mortality due to heatwave and its characteristics under climate change, population and adaptation scenarios. *Int. J. Hyg. Environ. Heal.* **250**, 114157 (2023).
35. Jones, B. & O'Neill, B. C. Spatially explicit global population scenarios consistent with the shared socioeconomic pathways. *Environ. Res. Lett.* **11**, 84003–84012 (2016).
36. Gasparrini, A., Armstrong, B. & Kenward, M. G. Distributed lag non-linear models. *Stat. Med.* **29**, 2224–2234 (2010).
37. Gasparrini, A. et al. Mortality risk attributable to high and low ambient temperature: a multicountry observational study. *Lancet* **386**, 369–375 (2015).
38. Vicedo-Cabrera, A. M., Sera, F. & Gasparrini, A. Hands-on tutorial on a modeling framework for projections of climate change impacts on health. *Epidemiology* **30**, 321–329 (2019).
39. Gasparrini, A., Armstrong, B. & Kenward, M. G. Multivariate meta-analysis for non-linear and other multi-parameter associations. *Stat. Med.* **31**, 3821–3839 (2012).
40. Verbeke G. & Molenberghs G. *Linear Mixed Models for Longitudinal Data* Vol. 7 (Springer Verlag: New York, 2000).

ACKNOWLEDGEMENTS

The study was supported by the Provincial Natural Science Foundation of Fujian Province (No. 2021J01728), the Guangdong Basic and Applied Basic Research Foundation (No. 2020A1515011161), the National Natural Science Foundation of China (No. 82003552) and the Start-up Funds for Introducing Talents to Fujian Medical University (No. XRCZX2020017). We greatly thank the China Meteorological Data Service Center, the Working Group on Coupled Modeling (WGCM), and the NCAR's IAM group and the City University of New York Institute for Demographic Research for the publicly available weather data, future temperature data and future spatial population data.

AUTHOR CONTRIBUTIONS

Z.-J.H., Z.-Y.Z. and J.Y. initiated this study. Z.-J.H., Z.-Q.Z. and D.-L.L. collected the data. Z.-Y.Z., X.Z. and D.-L.L. cleaned and analyzed the data. Z.-Y.Z., J.Y. and X.Z. drafted the manuscript with important inputs from Z.-J.H., Z.-Q.Z. and X.-X.X. Z.-Y.Z., J.Y. and X.Z. contributed equally and are considered as co-first author.

COMPETING INTERESTS

The authors declare no competing interests.

ADDITIONAL INFORMATION

Supplementary information The online version contains supplementary material available at <https://doi.org/10.1038/s41612-023-00439-7>.

Correspondence and requests for materials should be addressed to Zhi-Jian Hu.

Reprints and permission information is available at <http://www.nature.com/reprints>

Publisher's note Springer Nature remains neutral with regard to jurisdictional claims in published maps and institutional affiliations.



Open Access This article is licensed under a Creative Commons Attribution 4.0 International License, which permits use, sharing, adaptation, distribution and reproduction in any medium or format, as long as you give appropriate credit to the original author(s) and the source, provide a link to the Creative Commons license, and indicate if changes were made. The images or other third party material in this article are included in the article's Creative Commons license, unless indicated otherwise in a credit line to the material. If material is not included in the article's Creative Commons license and your intended use is not permitted by statutory regulation or exceeds the permitted use, you will need to obtain permission directly from the copyright holder. To view a copy of this license, visit <http://creativecommons.org/licenses/by/4.0/>.

© The Author(s) 2023